Profound Contrast Adaptation Early in the Visual Pathway

Samuel G. Solomon, Jonathan W. Peirce,
Neel T. Dhruv, and Peter Lennie*
Center for Neural Science
New York University
New York, New York 10003

Summary

Prior exposure to a moving grating of high contrast led to a substantial and persistent reduction in the contrast sensitivity of neurons in the lateral geniculate nucleus (LGN) of macaque. This slow contrast adaptation was potent in all magnocellular (M) cells but essentially absent in parvocellular (P) cells and neurons that received input from S cones. Simultaneous recordings of M cells and the potentials of ganglion cells driving them showed that adaptation originated in ganglion cells. As expected from the spatiotemporal tuning of M cells, adaptation was broadly tuned for spatial frequency and lacked orientation selectivity. Adaptation could be induced by high temporal frequencies to which cortical neurons do not respond, but not by low temporal frequencies that can strongly adapt cortical neurons. Our observations confirm that contrast adaptation occurs at multiple levels in the visual system, and they provide a new way to reveal the function and perceptual significance of the M pathway.

Introduction

The appearance of a pattern depends on the context in which it is viewed. Prolonged viewing of a simple pattern usually leads to a change in both its appearance and that of similar patterns viewed afterwards (Blakemore and Campbell, 1969), a phenomenon referred to as contrast adaptation. The aftereffects of adaptation are confined to patterns of similar orientation, and since orientation-selective mechanisms are not found before cortex (Hubel and Wiesel, 1962), contrast adaptation has been widely used in perceptual work to infer the properties of cortical feature analyzers (Graham, 1989). Consistent with this interpretation, early physiological studies that examined the effects of prolonged exposure to contrast patterns found no adaptation in the lateral geniculate nucleus (LGN) of cat (Maffei et al., 1973; Movshon and Lennie, 1979; Ohzawa et al., 1985; Shou et al., 1996) or monkey (Derrington et al., 1984), but did find substantial adaptation in orientation-selective cortical neurons in cat (Maffei et al., 1973; Movshon and Lennie, 1979; Ohzawa et al., 1985) and monkey (Carandini et al., 1998; Sclar et al., 1989).

Recent recordings have described a slow contrast adaptation in the retina of salamander (Kim and Rieke, 2001; Smirnakis et al., 1997), rabbit (Baccus and Meister, 2002; Brown and Masland, 2001), and macaque (Chander and Chichilnisky, 2001) and throw doubt on the usefulness

*Correspondence: pl@cns.nyu.edu

of contrast adaptation as a probe of cortical function. It is difficult to relate the new findings to those from psychophysics and cortical neurophysiology. First, the stimuli used in the retinal studies were spatially uniform fields or checkerboards whose luminance was rapidly and randomly modulated in time—quite different from the stimuli used in perceptual and cortical studies. Second, only one study (Chander and Chichilnisky, 2001) has investigated slow contrast adaptation in the primate retina, and that found substantially less adaptation than in the salamander. We describe here new observations that sharply clarify the picture in the primate visual pathway and have major implications for psychophysical studies: neurons in magnocellular LGN (M cells), but not those in parvocellular LGN (P cells), show strong contrast adaptation that originates in the retina.

Results

Aftereffects of Adaptation to High-Contrast Stimuli

We studied the responses of single neurons in LGN of anesthetized macaque before, during, and through recovery from adaptation to contrast modulation of different stimuli. Our initial experiments were prompted by observations in ganglion cells (Baccus and Meister, 2002; Chander and Chichilnisky, 2001; Kim and Rieke, 2001; Smirnakis et al., 1997) that when stimulated by temporal modulation of a spatially uniform field, the average discharge declined over several seconds. To explore this, we stimulated neurons by modulating the luminance of a spatially uniform achromatic patch displayed on a television monitor. The patch was considerably larger than the receptive field, on which it was centered, and was modulated in time by a binary noise sequence with a new sample on each displayed frame (90 Hz). Figure 1A shows the average discharge of an M cell before, during, and after a 20 s presentation of the noise. The noise had no immediate effect on the average discharge rate, but after its removal the maintained discharge to a blank screen was profoundly depressed for several seconds. Over all the 32 M cells characterized with noise stimuli, the average discharge declined slightly (19%) during stimulation, and the subsequent maintained discharge dropped by 57.0%, recovering with a time constant of 6.0 s. The modest decline in mean discharge rate during adaptation is about the same as that found by Chander and Chichilnisky (2001) among their more responsive monkey ganglion cells. The postadaptation drop in maintained discharge has not been described before; in the in vivo preparation, this is easily seen against the substantial maintained discharge, averaging 17 imp/s among our M cells in LGN (slightly lower than in counterpart ganglion cells; Troy and Lee, 1994).

Ganglion cells are better activated by spatially uniform fields than are LGN neurons (Kaplan et al., 1987), whose responses to such stimuli might never be strong enough to reveal changes brought about by adaptation. We therefore explored adaptation to high-contrast moving
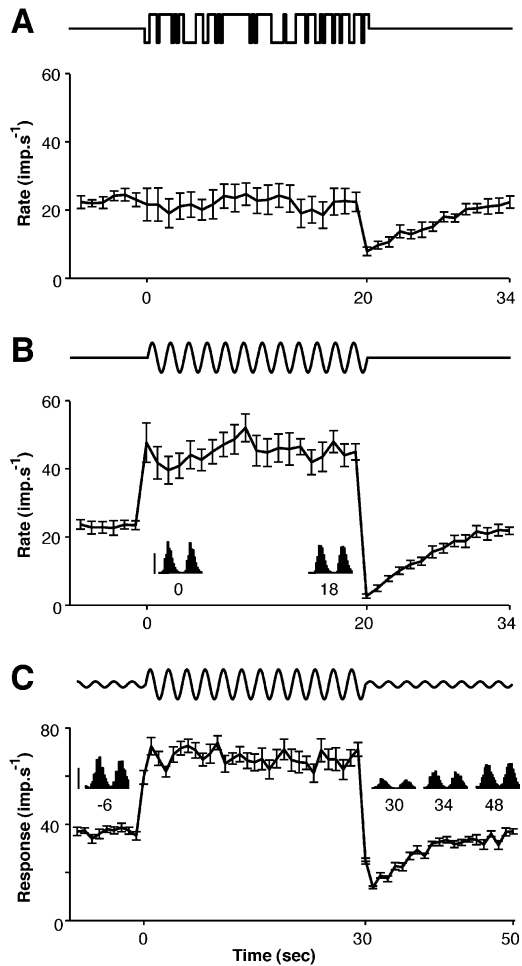
Figure 1. Effect of Prolonged Exposure to a High-Contrast Stimulus on the Discharge of an Off-Center M Cell

(A) Average discharge rate before, during, and after 20 s of binary noise modulation (100%) of a spatially uniform field at 90 Hz. Before and after stimulation, the screen displayed a uniform field at the mean luminance (55 cd.m^{-2}). Error bars show ±2 standard errors of the mean, which is based on 14 stimulus cycles. The trace above the plot shows schematically the temporal luminance profile of the stimulus.

(B) Average discharge rate before, during, and after a 20 s presentation of a grating of optimal spatial frequency (100% contrast) moving at 11 Hz. Inset histograms show the modulation of discharge during the first 2 s and last 2 s. Vertical scale represents 100 impulses/s. Other details as for (A).

(C) Amplitude of modulated response at the frequency of stimulation before, during, and after presentation of a unit contrast grating of optimal spatial frequency, moving at 11 Hz. Before and after this presentation, grating contrast was fixed at 0.08. Inset histograms show the discharge sampled in 2 s epochs starting at the specified times before and after presentation of the high-contrast grating. Vertical scale represents 50 impulses/s.

gratings—very effective stimuli for both ganglion cells and LGN neurons, and potent stimuli to adaptation in cortical cells (Movshon and Lennie, 1979; Sclar et al., 1989). We used gratings of optimal spatial frequency, moving at a rate close to optimal for each cell (usually 11 Hz). The trace in Figure 1B shows the average discharge rate of the M cell of Figure 1A, measured in successive 1 s epochs during repeated 20 s presenta-

tions of a grating of unit contrast. The screen was blank at the mean luminance for 20 s between each presentation. The response declined negligibly over the adapting period, but after grating offset, the maintained discharge dropped just as it did following noise stimulation and recovered with the same time course. This occurred in all M cells.

The drop in the maintained discharge caused by adaptation was accompanied by markedly reduced responsivity. This was readily revealed by measuring the response to a low-contrast test grating, otherwise identical to the adapting grating, before and after adaptation. Figure 1C shows this for the cell of Figures 1A and 1B (Sanchez-Vives et al., 2000, found the same in some LGN cells in cat). In this as in all M cells, the response amplitude (first harmonic) was greatly depressed by adaptation; it recovered with the same time course as the maintained discharge. In 11 M cells (not shown), we explored the effects of adapting to a range of contrasts: adapting gratings were generally ineffective unless their contrasts exceeded 0.15 (a contrast that evokes strong, rectified, but not yet saturating responses), and the effectiveness of the adaptor increased with contrast. Yet at no contrast did the response to the adapting grating decline substantially during the adapting period. This apparent paradox most likely reflects the saturation of responses to contrasts above about 0.2: adaptation at any particular contrast is never strong enough to bring the response out of saturation.

Modeling the Change in Response

The loss of response to weak stimuli might reflect either a change in contrast gain or an increase in the neuron's threshold for generating action potentials (hyperpolarization), resulting in greater rectification of responses (e.g., Kim and Rieke, 2001). To determine how these two factors contributed to the changes in responses, we adopted a simple model of the light response in which the membrane potential varies linearly with the light signal and firing rate at any instant is a nonlinear function of that generator potential (see Experimental Procedures). The form of the nonlinearity does not depend on the state of adaptation.

We fit this model to 2 s segments of the average responses to low-contrast gratings, obtained immediately after offset of the adapting stimulus and then 18 s later (Figure 2A). Smooth lines show the model fit for the cell of Figure 1, obtained with only the mean generator potential (A) allowed to vary between conditions. In the unadapted state, the response was nearly sinusoidally modulated around a mean, with no rectification, but in the adapted state the response was strongly rectified. We used the model to characterize the responses of 31 M cells, first allowing only the mean (A) term of the spike generator signal to vary between unadapted and adapted states. Over our sample of M cells, the model accounted for 89.6% (SD 7.1%) of the variance in response (see Experimental Procedures). When we allowed the gain of the generator signal (G) also to vary between the two states, the fits did not improve. This suggests that contrast adaptation reflects predominantly a change in the mean membrane potential.

To understand how generally useful the model could
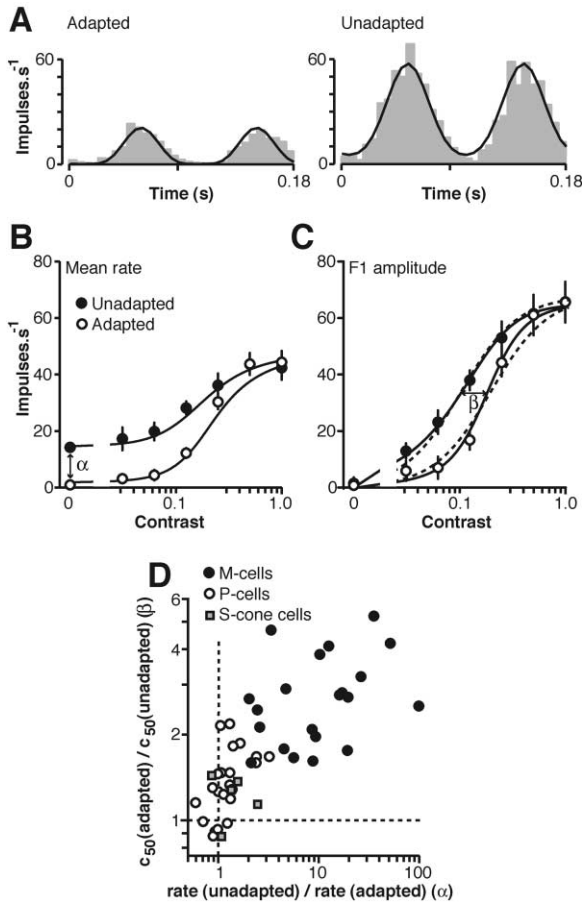
Figure 2. Effect of Adaptation on Average Discharge Rate and Response Gain

(A) Shaded histograms show the modulation of discharge in response to a drifting grating of contrast 0.08 sampled in 2 s epochs immediately after adaptation to high-contrast gratings ("adapted") and 18 s later ("unadapted"). Both adapting and test gratings moved at 11 Hz; histograms are folded to 2 stimulus cycles. The smooth lines show the best-fitting solutions to Equation 3, with only the mean membrane potential allowed to vary between unadapted and adapted states.

(B) The mean discharge rate as a function of contrast when the neuron was unadapted (filled circles) and adapted to unit contrast (open circles). Solid lines show best-fitting predictions of Equation 4 when only the mean membrane potential differs between adapted and unadapted states.

(C) Same as (B), but symbols and predictions show the amplitude (F1) of the modulated discharge rate at the temporal frequency of stimulation. Dashed lines show the best-fitting predictions to Equation 1 when only c_{50} was allowed to change. Parameters for the model in (B) and (C): G, 71.3; R_{max}, 102.2; g_{50}, 16.0; n, 4.3; A (unadapted), 10.7; A (adapted), 6.1.

(D) Comparison of the change in the maintained discharge rate (α) with the change in the contrast gain (β) for the neurons in our sample, obtained as shown in (B) and (C) (n = 48). The dashed lines show where points would lie if adaptation had no effect.

be, we measured the effects of adaptation on responses to gratings of different contrasts. During prolonged exposure to a high-contrast grating, and starting after an initial 30 s, we substituted a 0.5 s test probe of different contrast every 5.5 s. This allowed us to construct contrast-response curves for the adapted state that could

be compared with others obtained before adaptation and after recovery. For the cell of Figures 1 and 2A, Figures 2B and 2C show, respectively, how adaptation affected the mean discharge rate and the amplitude of the first harmonic component of response. Adaptation brought about a profound drop in the maintained firing rate (Figure 2B) and apparently a drop in the contrast gain (Figure 2C) but had no effect on the maximum response of the neuron. The solid lines in Figures 2B and 2C show the fits of Equation 4 (Experimental Procedures) when only the mean generator signal (A) was allowed to vary between the unadapted and adapted states. Allowing the gain of the generator signal (G) also to vary did not improve the fit. Across the 22 M cells on which we made measurements, allowing the gain term to vary improved the fit in 7 of the cells. It is important to note, however, that in the adapted state the maintained discharge rate is very low, and the estimate of mean generator signal is poorly constrained. We do not know if better-constrained values would entail a larger change in gain. If we consider only the effect of adaptation on the modulated response, contrast-response relationships can be well fit by allowing only the contrast gain to vary (dashed lines in Figure 2C).

Although our modeling suggests that much of contrast adaptation can be explained by a change in mean membrane potential, measurements obtained with extracellular recordings do not tightly constrain the contribution. Experimentally, the effects of adaptation can be captured by characterizing either the change in the rate of maintained discharge or the change in contrast gain—the contrast eliciting half the maximal modulated response (c_{50}; the maximum response was that elicited by a contrast of 1.0 in the unadapted state). Figure 2D shows the ratio of contrast gains (β, Figure 2C) plotted against the change in maintained discharge (α, Figure 2B) for the 22 M cells on which we made measurements and also for 21 P cells and 5 cells with strong S cone input. Among the M cells, adaptation reduced the average maintained discharge from 17.3 imp/s to 4.2 imp/s and increased the average contrast gain from 0.11 to 0.28. The large changes in maintained discharge and contrast gain that characterize adaptation in M cells were absent, or nearly so, in most P cells: the average maintained discharge fell from 16.3 imp/s to 14.5 imp/s, and average contrast gain rose from 0.35 to 0.47. For the S cone cells (all S-On), average contrast gain rose from 0.31 to 0.37, and maintained discharge fell from 14.0 imp/s to 10.9 imp/s.

Given two comparable measures of adaptation (Figure 2D), the change in contrast gain commends itself as more generally useful: over the full range of stimulus contrasts, it is better constrained by our measurements; it will reveal adaptation whether or not the maintained discharge changes; and it permits our results to be compared with those of previous studies, notably those involving cortical neurons, which often have no maintained discharge.

Effect of Adaptation on Contrast Gain
Figure 3A shows how the average modulated response (unadapted and adapted) grew with contrast for the 22 M cells we studied. To characterize the change in contrast gain, we fitted contrast-response curves with a reduced form of the model of the light response:
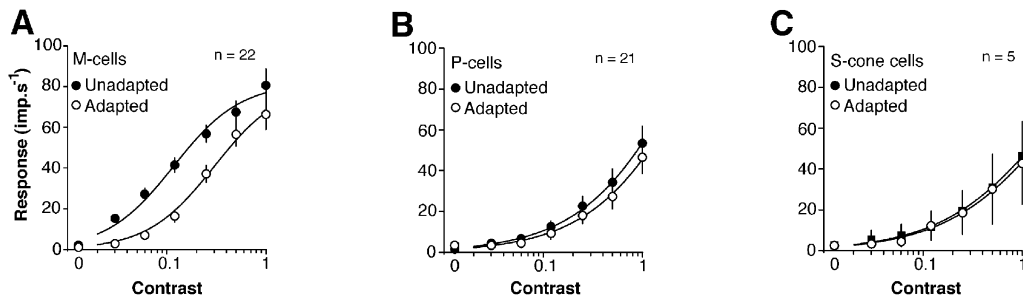
Figure 3. How Adaptation Affects the Growth of Response with Stimulus Contrast

(A) Average modulation of the discharge measured in 0.5 s samples of response from 22 M cells driven by achromatic gratings of optimal spatial frequency and temporal frequency of 9 or 11 Hz. Open circles show the amplitude of response when cells were adapted to a unit contrast grating with the same spatial and temporal properties as the test; filled circles show the amplitude of response in the unadapted state (average of two sets of measurements, one made immediately before adaptation and the other made 2 min after adaptation). Smooth curves drawn through both sets of points are concurrently fitted solutions to Equation 1, with only c_{50} allowed to be different. Vertical bars show ± 2 standard errors of the mean.

(B) Average curves obtained from 21 P cells. For each cell, measurements were made with achromatic gratings of optimal spatial frequency moving at between 6 and 11 Hz. Conventions as in (A).

(C) Average curves obtained from 5 S cone cells (all S-On). For each cell, measurements were made with achromatic gratings of optimal spatial frequency moving at between 6 and 11 Hz. Conventions as in (A).

$$R = R_{max}\frac{c^n}{c_{50}^n + c^n}, \qquad (1)$$

where c is stimulus contrast, R is the amplitude of the first harmonic component of response, R_{max} is the asymptotic response to a high-contrast stimulus, and n and c_{50} define, respectively, the steepest slope of the contrast-response function and the contrast at half-maximum response (the contrast gain). When all three parameters in Equation 1 were allowed to vary between unadapted and adapted states, the best-fitting solutions accounted for 99.4% of variance in the responses of our sample of M cells (see Experimental Procedures). When only c_{50} was allowed to vary between states, the best-fitting solutions accounted for 97.7% of the variance. Smooth curves in Figure 3 are best-fitting solutions to Equation 1 when only c_{50} was allowed to vary. The difference between the curves in Figure 3A is well described by an increase in c_{50} from 0.12 to 0.31.

We also characterized adaptation in 21 P cells and in 5 S cone recipient cells that lay in interlaminar regions. Among the P cells, the average amplitude of the response to a high-contrast grating fell 7.6% (SD 10%) during prolonged stimulation. Among cells where the maintained discharge and contrast gain changed enough to be characterized, the time course of recovery was the same as in M cells (6–7 s). Adaptation caused a small change in contrast gain in 11 of 21 P cells. Figure 3B shows the average contrast-response curves before and during adaptation. Because responses did not saturate, fits of Equation 1 are poorly constrained (see Experimental Procedures). With only c_{50} allowed to vary between states (curves shown), it changed from 0.19 to 0.27. Among the five neurons that received input from S cones (all S-On), we saw even less adaptation than in P cells (Figure 3C).

tecting a subsequently viewed pattern, but to establish how much this threshold will change we need to consider not just the reduction in contrast gain but also the noisiness of discharge, which adaptation might also alter. Among M cells we found that adaptation did alter the variability of the discharge, but only at low contrasts: the ratio of response variance to response mean at a contrast of 0.03 was 3.1 in the unadapted state and 4.73 in the adapted state, but was 3.9 (unadapted) and 4.1 (adapted) at a contrast of 0.25. To represent the combined effects of reduced sensitivity and increased noise, we used signal detection theory (see Experimental Procedures) to estimate the contrast at which the stimuli could be reliably detected (probability of 0.75) before adaptation and during it. In the unadapted state, many M cells (14/22) could detect the lowest contrast (0.03) we used, but by extrapolating contrast-response relationships (see Experimental Procedures), we estimated threshold to be close to 0.023. In the adapted state, threshold was on average 0.093—a 4-fold increase. At high contrasts, where cortical neurons often give saturating responses, the loss of sensitivity caused by adaptation can be beneficial if it brings otherwise saturating contrasts within the cell's operating range without increasing the response variance (Ohzawa et al., 1985; Sclar et al., 1989). This was also the case for the M cells we studied. We estimated the discriminability (d') (Green and Swets, 1966) between gratings of contrasts 0.25 and 0.5, before and during adaptation. Adaptation increased discriminability: across our sample of 22 M cells, average d' was 0.88 before adaptation and 1.74 during adaptation (p < 0.001, paired t test). Among the 11 P cells in which adaptation caused any loss of contrast sensitivity, adaptation slightly increased the detection threshold, without improving the discriminability of high-contrast gratings.

Effect of Adaptation on Contrast Detection and Discrimination
The change in contrast gain (c_{50}) brought about by adaptation will increase a cell's contrast threshold for de-

Stimulus Specificity and Locus of Contrast Adaptation
In most M cells, we measured the effects of adaptation to gratings of different contrasts and several spatial
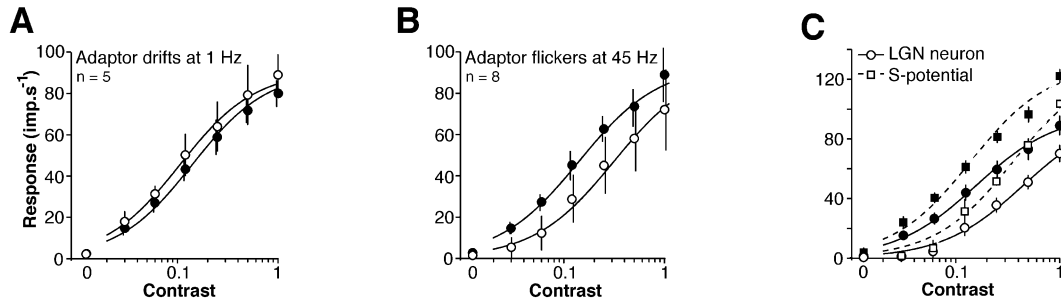
Figure 4. Stimulus Specificity of Adaptation

(A and B) Contrast-response curves for gratings of optimal spatial frequency drifting at 11 Hz, unadapted, and following adaptation to a grating drifting at 1 Hz (A), or counter-phase flickering at 45 Hz in the maximally effective phase (B). Conventions as in Figure 3.

(C) Retinal origin of adaptation. Solid curves and circles show the effects of adaptation on the responses of an M cell. Dashed curves and squares characterize the responses of concurrently recorded S potentials that reflected ganglion cell input. Conventions as in Figure 3.

and temporal frequencies, testing with a grating of near optimal spatial and temporal frequency (Figures 4A and 4B and Table 1). The effectiveness of the adaptor was generally predicted by the spatiotemporal tuning of the cells. Since M cells lack orientation or direction specificity, adapters were equally effective regardless of their direction of movement (Table 1). Further, M cells respond very well to stimuli modulated at high temporal frequencies (Derrington and Lennie, 1984; Lee et al., 1990), which were potent adapters (Figure 4B), but much less well to those modulated at low temporal frequencies, which were poor adapters (Figure 4A). The exception to this general rule was adaptation to temporally modulated uniform fields: by comparison with other suboptimal adapting stimuli that evoked responses of similar amplitude, this caused a disproportionately large reduction in response to the test grating (Table 1). We think this happens because adaptation observed in LGN originates in retinal ganglion cells, which are relatively more responsive to (and therefore readily adapted by) spatially uniform fields (Kaplan et al., 1987). We obtained direct evidence on the retinal origin of adaptation from three M cells for which we were able to record, concur-

rently with the action potentials, the so-called S potentials that reflect the driving inputs from ganglion cells (Bishop et al., 1962; Kaplan and Shapley, 1984). Figure 4C shows contrast-response curves for one such neuron (solid lines and circles) and its S potential (dashed lines and squares). The data from the S potentials were well fit by a shift in c_{50} from 0.14 to 0.35. The c_{50} of the target M cell shifted from 0.16 to 0.44. In this and in the two other S potential-LGN pairs we recorded, the effects of adaptation in LGN (including the postadaptation drop in maintained discharge) were substantially accounted for by the change observed in the retinal ganglion cell.

The very different effects of contrast adaptation on M and P cells suggest that the adaptation occurs after the M and P pathways diverge, but we do not know that it originates in ganglion cells. Some additional results bear on this question. When the adapting pattern was presented to an M cell as a counterphase-flickering grating in the spatial phase for peak response, it had the expected effect on the contrast-response curve, but when presented in the phase for null response it did not adapt the cell. This must mean that adaptation arises at or after the site of spatial pooling within the ganglion

Table 1. The Effect of Adaptation on the Contrast-Response Functions of M Cells in the LGN

| Adapting Condition[a] | Number of Cells[b] | Relative Response to Adapter[c,d] | Percent Change in Parameter[d] | | R_{max} Fixed |
| | | | All Parameters Allowed to Vary | | |
			c_{50}	R_{max}	c_{50}
Optimal configuration	22	-	78.3 (15.53)	−15.8 (4.55)	177.7 (22.26)
Different direction	7	0.99 (0.05)	84.4 (22.36)	−17.8 (8.44)	211.2 (48.69)
Uniform field	8	0.54 (0.08)	109.6 (26.05)	0.4 (4.88)	122.9 (24.72)
Contrast 0.1	7	0.60 (0.06)	10.3 (10.46)	6.0 (4.11)	6.8 (13.23)
Contrast 0.5	4	0.93 (0.08)	32.7 (33.39)	−23.7 (6.66)	116.9 (54.02)
1 Hz	5	0.43 (0.04)	−0.1 (8.62)	12.2 (8.53)	−16.5 (17.26)
45 Hz	8	0.82 (0.06)	69.2 (37.36)	−9.5 (15.81)	301.1 (158.85)

[a] In the base adapting condition (optimal configuration), adapters were of the optimal spatial and temporal frequency for the cell, at a contrast of 1.0. Other adapting conditions differed from the base condition as follows. To test the orientation and direction specificity of adaptation (different direction), we used adapting gratings that were either orthogonal to, or moved in the opposite direction to, the test grating. To explore the effect of low spatial frequency adapters, we used spatially uniform fields modulated at the same temporal frequency as the test (uniform field). To explore the effect of adapting contrast, we used contrasts of 0.1 and 0.5. To explore the temporal frequency tuning of adaptation, we used adapting gratings moving at 1 Hz or counter-phase modulated at 45 Hz in the optimum spatial phase.
[b] Not all cells were tested with all adapting stimuli.
[c] For each adapting condition, values show the ratio of the response obtained in that condition to the response to the optimal adaptor.
[d] Values in parentheses show the standard error of the mean.

cell's receptive field. At the eccentricities we explored, M (parasol) ganglion cells pool signals from at least 30–50 diffuse bipolar cells (Jacoby et al., 2000), so it seems unlikely that the site of adaptation could be earlier than the inner plexiform layer (Baccus and Meister, 2002; Kim and Rieke, 2001).

Discussion

Baccus and Meister (2002) showed that contrast adaptation in the retina can be separated into two components—one fast and one slow. The fast component is essentially instantaneous and is evident in changes in both the gain and temporal response of ganglion cells (cf. Shapley and Victor, 1978). This type of contrast adaptation is absent from P cells of the macaque retina and LGN (Benardete and Kaplan, 1997) but is robust in M cells. The slow component, which we show to be robust in M cells and weak or absent in P cells, seems to reduce gain without altering the temporal response (Baccus and Meister, 2002). While the slow adaptation in M cells resembles that found in the retina using rapid random temporal modulation of uniform fields, several of our observations are new. We found profound depression of the maintained discharge, something that has not been investigated in retinal work. We found little reduction in the response to prolonged stimulation with high-contrast stimuli (Figure 1), which has been the focus of most retinal studies. Species differences might account for some of this: Chander and Chichilnisky (2001) (Figure 2) found that among their most responsive primate ganglion cells, the average discharge rate fell by about 20%—the same amount we found, and very much less than in salamander ganglion cells. Finally, we found a profound loss of responsivity to stimuli of low contrast (e.g., Figure 1C).

Given the powerful contrast adaptation in M cells, it might seem puzzling that previous work failed to find it. Earlier work on macaque LGN (Derrington et al., 1984) focused on P cells and used low temporal frequencies that are relatively ineffective adapters even in M cells. But perhaps most important, even in M cells the common measure of adaptation—a decline in response to prolonged high-contrast stimulation—reveals little about what is changed (Figures 1B and 1C). The failure to find consequential adaptation in cat LGN (Maffei et al., 1973; Movshon and Lennie, 1979; Ohzawa et al., 1985; Sanchez-Vives et al., 2000; Shou et al., 1996) might to some extent stem from the use of low temporal frequency adapting stimuli, though it is worth noting that in experiments that resembled ours and explored a wide range of temporal frequencies, V. Mante and M. Carandini (personal communication) found no adaptation in cat.

Since the adaptation we have described in M cells is broadly tuned in spatial and temporal frequency and is not orientation selective, we might expect to find a correspondingly broadly tuned expression of it in cortical neurons and in perception. Physiological work on cortex has generally shown the converse: aftereffects are confined to spatial patterns resembling the adapting pattern (Carandini et al., 1998; Movshon and Lennie, 1979; Müller et al., 1999). This might mean that the M pathway has no influence on cortical neurons that adapt

to contrast. However, we have shown that gratings modulated at low temporal frequencies do not adapt M cells, and it is just these frequencies that are usually used to study contrast adaptation in cortical neurons.

Our findings suggest that perceptual adaptation to patterns moving at high temporal frequencies, which favor M cells, should have a substantial component that is not orientation selective. This is in fact the case: adaptation to patterns of low spatial frequency moving at 15 Hz is not orientation selective at all (Kelly and Burbeck, 1987). M cells respond to stimuli modulated at temporal frequencies higher than can be perceived (Lee et al., 1990) and above those to which most neurons in V1 respond (Hawken et al., 1996). Adaptation in M cells, therefore, probably explains why perceptual adaptation to high-contrast stimuli modulated at invisibly high rates reduces contrast sensitivity to stimuli modulated at lower temporal frequencies (Shady et al., 2004).

Our finding of strong adaptation in M cells but not P cells, coupled with the knowledge that M cells are substantially more sensitive than are P cells to stimuli modulated at high temporal frequency (Derrington and Lennie, 1984; Lee et al., 1994), offers a powerful new approach to discovering the breadth of the M pathway's perceptual influence: one could examine an observer's sensitivity to stimuli that drive the P pathway well, before and following adaptation to rapidly moving or flickering stimuli that excite M cells well but are imperceptible or almost so.

Experimental Procedures

Single unit recordings were made from the LGN in five anesthetized, paralyzed male *M. fascicularis*, prepared as described (Solomon et al., 2004). A craniotomy 10 mm in diameter was made over the right LGN, and a guide tube containing the electrode was placed stereotaxically with its tip 3 mm above the LGN. The experiments reported here were part of a larger set in which we wanted recordings from neurons with receptive fields in near peripheral retina. Neurons characterized in the present work had receptive fields between 5° and 25° from the fovea.

Achromatic gratings were displayed on a calibrated monitor (Sony G500 or Eizo T966) with a frame rate of 90 Hz and a mean luminance of 55 cd.m^{-2}. The monkey viewed this through dilated pupils (~7 mm dia). To prevent drift, the eyes were stabilized with fixation rings (Duckworth & Kent Ltd, Baldock, UK).

Measuring Contrast-Response Functions
Contrast-response functions for drifting gratings of optimal spatial and temporal frequency were obtained before, during, and after recovery from adaptation to different adapting stimuli. In making measurements before and after recovery, each grating was presented for 0.5 s, with 0.5 s blank between presentations; the time-averaged Michelson contrast was 0.16. In making measurements during adaptation, each test grating was presented for 0.5 s, separated by 5 s adaptation, after an initial adapting period of 30 s. A complete data set contained responses to 20 presentations of each test grating. From the averaged response to all presentations of a particular stimulus, we extracted the mean discharge rate and the amplitude of the Fourier component at the frequency of modulation. For each cell we combined the measurements made before and after recovery and compared this combined "unadapted" measure to that obtained in the adapted state.

Model of Light Response
We fit a simple model of light response to histograms of firing rates obtained for single contrast values (Figure 2A) and to the two sets of contrast-response curves (Figures 2B and 2C). The linear-nonlinear

cascade (LN) model is like that of Chander and Chichilnisky (2001) and Kim and Rieke (2001). For sinusoidal modulation in time, we represent the ganglion cell's spike generator signal (*g*) as a sinusoidal modulation around a mean followed by rectification:

$$f(ø) = A + G \cdot c \sin(ø + p) \qquad (2)$$

$$g(ø) = \max(f(ø),0), \qquad (3)$$

where *ø* is the temporal phase of the grating, *A* is the resting generator signal, *c* is the amplitude of modulation (contrast) of the stimulus, *G* is the contrast gain of the generator signal, and *p* is a phase offset. The rectification step in Equation 3 mimics a hard threshold for the production of spikes. The relationship between the generator signal and spike rate *R* is given by

$$R(ø) = R_{max} \frac{g(ø)^n}{g_{50}^n + g(ø)^n}, \qquad (4)$$

where R_{max} is the maximum firing rate, g_{50} is the generator signal that brings about half maximum firing rate, and *n* is an output exponent. The terms $g(ø)$ and g_{50} are inseparable: a doubling of $g(ø)$ can be compensated by a doubling of g_{50}. The absolute values of the parameters *A*, *G*, and g_{50} are therefore poorly constrained; the relative values of *A* and *G* in the two states are, however, unique solutions. The model does not explicitly incorporate a rapid contrast gain control (Baccus and Meister, 2002; Benardete et al., 1992; Shapley and Victor, 1979) and thus does not explain the advance in response phase (which we saw in both the adapted and unadapted states) as contrast increases. However, the effects of this rapid gain-control on responsivity are absorbed in Equation 4.

Characterizing Contrast-Response Functions

To characterize the changes in the modulated response brought about by adaptation, we fit Equation 1 independently to the unadapted and adapted responses, and also concurrently to the same responses, in the latter case allowing only c_{50}, or only R_{max}, to differ between conditions.

For M cells, where responses were usually saturated at high contrasts, parameter values were well constrained. In 20 of 22 cells, the curves were better described by a change in c_{50} than a change in R_{max}: fixing c_{50} accounted for an average of 95.0% (SD 2.74) of the variance (calculated as described in Carandini et al., 1997) and fixing R_{max} accounted for 97.3% (SD 1.6) of the variance. In Table 1 we give the estimate of the percent shift in c_{50} brought about by each adaptation condition, when all parameters were allowed to vary, and when only the c_{50} was allowed to vary. For P cells, the curves could be equally well described by a small change in either parameter: fixing c_{50} accounted for an average of 98.0% (SD 1.5) of the variance and fixing R_{max} accounted for 97.6% (SD 2.0) of the variance.

Estimating Contrast at Detection Threshold

Since most M cells could detect gratings at the lowest contrast we presented, we needed a method for extrapolating response and response variability. We used a bootstrap analysis for this. For each of the n trials (generally 20) on which a grating had been presented at a particular contrast, we estimated the first Fourier component of response. For each of 1000 repetitions, we then drew (with replacement) n responses from this set of trials and calculated the mean of each new, randomly chosen, set. This left us with a thousand estimates of mean response at each of seven contrasts from 0 to 1. We then randomly selected one of these thousand estimates at each contrast and fit that set of responses with Equation 1, except that we added a new term (*M*) that allowed for a maintained discharge:

$$R = R_{max} \frac{c^n}{c_{50}^n + c^n} + M. \qquad (5)$$

(*M* is required because the amplitude of the first Fourier component of response computed on a single trial is contaminated by variation in the maintained discharge in a way that it is not when computed from the averaged response to all trials—see Forte et al., 2002.) We repeated this for each of the thousand estimates of mean rate that

we had. From these bootstrapped fits, we were able to estimate the mean and variance of response, and of the maintained discharge, at arbitrary contrast levels from 0 to 1.

Estimating Discriminability of Responses

To estimate contrast threshold, we generated receiver-operator characteristic (ROC) (Tolhurst et al., 1983) curves for each cell from responses derived by the bootstrap procedure described above. The probability of detection at a particular contrast is determined by how much the distribution of bootstrapped responses overlaps that for maintained discharge to a gray screen.

To estimate *d′*, we follow Green and Swets (1966):

$$d' = \frac{\mu_1 - \mu_2}{\sqrt{(\sigma_1^2 + \sigma_2^2)/2}}, \qquad (6)$$

where μ_1 and μ_2 are the measured mean response rates at the two contrasts, and σ_1^2 and σ_2^2 are the corresponding variances.

References

Baccus, S.A., and Meister, M. (2002). Fast and slow contrast adaptation in retinal circuitry. Neuron *36*, 909–919.

Benardete, E.A., and Kaplan, E. (1997). The receptive field of the primate P retinal ganglion cell. II: Nonlinear dynamics. Vis. Neurosci. *14*, 187–205.

Benardete, E.A., Kaplan, E., and Knight, B.W. (1992). Contrast gain control in the primate retina: P cells are not X-like, some M cells are. Vis. Neurosci. *8*, 483–486.

Bishop, P.O., Burke, W., and Davis, R. (1962). The interpretation of the extracellular response of single lateral geniculate cells. J. Physiol. *162*, 451–472.

Blakemore, C., and Campbell, F.W. (1969). On the existence of neurones in the human visual system selectively sensitive to the orientation and size of retinal images. J. Physiol. *203*, 237–260.

Brown, S.P., and Masland, R.H. (2001). Spatial scale and cellular substrate of contrast adaptation by retinal ganglion cells. Nat. Neurosci. *4*, 44–51.

Carandini, M., Heeger, D.J., and Movshon, J.A. (1997). Linearity and normalization in simple cells of the macaque primary visual cortex. J. Neurosci. *17*, 8621–8644.

Carandini, M., Movshon, J.A., and Ferster, D. (1998). Pattern adaptation and cross-orientation interactions in the primary visual cortex. Neuropharmacology *37*, 501–511.

Chander, D., and Chichilnisky, E.J. (2001). Adaptation to temporal contrast in primate and salamander retina. J. Neurosci. *21*, 9904–9916.

Derrington, A.M., and Lennie, P. (1984). Spatial and temporal contrast sensitivities of neurones in lateral geniculate nucleus of macaque. J. Physiol. *357*, 219–240.

Derrington, A.M., Krauskopf, J., and Lennie, P. (1984). Chromatic mechanisms in lateral geniculate nucleus of macaque. J. Physiol. *357*, 241–265.

Forte, J., Peirce, J.W., Kraft, J.M., Krauskopf, J., and Lennie, P. (2002). Residual eye-movements in macaque and their effects on visual responses of neurons. Vis. Neurosci. *19*, 31–38.

Graham, N. (1989). Visual Pattern Analyzers (New York: Oxford University Press).

Green, D.M., and Swets, J.A. (1966). Signal Detection Theory and Psychophysics (New York: Wiley).

Hawken, M.J., Shapley, R.M., and Grosof, D.H. (1996). Temporal-frequency selectivity in monkey visual cortex. Vis. Neurosci. *13*, 477–492.

Hubel, D.H., and Wiesel, T.N. (1962). Receptive fields, binocular interactions, and functional architecture in the cat's visual cortex. J. Physiol. *160*, 106–154.

Jacoby, R.A., Wiechmann, A.F., Amara, S.G., Leighton, B.H., and Marshak, D.W. (2000). Diffuse bipolar cells provide input to OFF parasol ganglion cells in the macaque retina. J. Comp. Neurol. *416*, 6–18.

Kaplan, E., and Shapley, R. (1984). The origin of the S (Slow) potential in the mammalian lateral geniculate nucleus. Exp. Brain Res. *55*, 111–116.

Kaplan, E., Purpura, K., and Shapley, R.M. (1987). Contrast affects the transmission of visual information through the mammalian lateral geniculate nucleus. J. Physiol. *391*, 267–288.

Kelly, D.H., and Burbeck, C.A. (1987). Further evidence for a broadband, isotropic mechanism sensitive to high-velocity stimuli. Vision Res. *27*, 1527–1537.

Kim, K.J., and Rieke, F. (2001). Temporal contrast adaptation in the input and output signals of salamander retinal ganglion cells. J. Neurosci. *21*, 287–299.

Lee, B.B., Pokorny, J., Smith, V.C., Martin, P.R., and Valberg, A. (1990). Luminance and chromatic modulation sensitivity of macaque ganglion cells and human observers. J. Opt. Soc. Am. A *7*, 2223–2236.

Lee, B.B., Pokorny, J., Smith, V.C., and Kremers, J. (1994). Responses to pulses and sinusoids in macaque ganglion cells. Vision Res. *34*, 3081–3096.

Maffei, L., Fiorentini, A., and Bisti, S. (1973). Neural correlate of perceptual adaptation to gratings. Science *182*, 1036–1038.

Movshon, J.A., and Lennie, P. (1979). Pattern-selective adaptation in visual cortical neurones. Nature *278*, 850–852.

Müller, J.R., Metha, A.B., Krauskopf, J., and Lennie, P. (1999). Rapid adaptation in visual cortex to the structure of images. Science *285*, 1405–1408.

Ohzawa, I., Sclar, G., and Freeman, R.D. (1985). Contrast gain control in the cat's visual system. J. Neurophysiol. *54*, 651–667.

Sanchez-Vives, M.V., Nowak, L.G., and McCormick, D.A. (2000). Membrane mechanisms underlying contrast adaptation in cat area 17 in vivo. J. Neurosci. *20*, 4267–4285.

Sclar, G., Lennie, P., and DePriest, D.D. (1989). Contrast adaptation in striate cortex of macaque. Vision Res. *29*, 747–755.

Shady, S., MacLeod, D.I.A., and Fisher, H.S. (2004). Adaptation from invisible flicker. Proc. Natl. Acad. Sci. USA, in press.

Shapley, R.M., and Victor, J.D. (1978). The effect of contrast on the transfer properties of cat retinal ganglion cells. J. Physiol. *285*, 275–298.

Shapley, R., and Victor, J.D. (1979). The contrast gain control of the cat retina. Vision Res. *19*, 431–434.

Shou, T., Li, X., Zhou, Y., and Hu, B. (1996). Adaptation of visually evoked responses of relay cells in the dorsal lateral geniculate nucleus of the cat following prolonged exposure to drifting gratings. Vis. Neurosci. *13*, 605–613.

Smirnakis, S.M., Berry, M.J., Warland, D.K., Bialek, W., and Meister, M. (1997). Adaptation of retinal processing to image contrast and spatial scale. Nature *386*, 69–73.

Solomon, S.G., Peirce, J.W., and Lennie, P. (2004). The impact of suppressive surrounds on chromatic properties of cortical neurons. J. Neurosci. *24*, 148–160.

Tolhurst, D.J., Movshon, J.A., and Dean, A.F. (1983). The statistical reliability of signals in single neurons in cat and monkey visual cortex. Vision Res. *23*, 775–786.

Troy, J.B., and Lee, B.B. (1994). Steady discharges of macaque retinal ganglion cells. Vis. Neurosci. *11*, 111–118.